Energy harvesting from human motion and bridge vibrations: an evaluation of current nonlinear energy harvesting solutions

P L Green, E Papatheou, N D Sims

1 Abstract

A large quantity of recent research into the harvesting of electrical energy from ambient vibration sources has been focused on the improvement of device performance via the deliberate introduction of dynamic nonlinearities. As well as this, the realisation that most of these kinetic energy sources are stochastic in nature has led to many works focusing on the response of energy harvesters to random vibrations (often Gaussian white noise). This differs from early work in which it was assumed that ambient vibration sources were sinusoidal. The aim of the present study is to take current nonlinear energy harvesting solutions and to numerically analyse their effectiveness when two real ambient vibration sources are used: human walking motion and the oscillation of the midspan of a suspension bridge. This work shows that the potential improvements that can be realised through the introduction of nonlinearities into energy harvesters are sensitive to the type of ambient excitation to which they are subjected. Additionally, the need for more research into the development of low frequency energy harvesters is emphasised.

2 Introduction

Much of the early work on energy harvesting was focused on the response of 'linear resonant' (LR) devices to sinusoidal excitations. Among the earliest, Williams and Yates (1996) proposed a device which was essentially a single-degree-of-freedom (SDOF) mass-spring-damper system where the viscous damper represented the transfer of energy from the mechanical to the electrical domain. Mitcheson et al. (2004) compared the response of Coulomb damped and velocity damped LR generators while, in (Stephen, 2006), work was focused on maximising the power that such a device can deliver to a load resistor. For a review of early energy harvester designs the work of Beeby, Tudor, and White (2006) is recommended.

From the above-mentioned works it was soon established that LR devices have two main limitations:

1. Size: with advances in microelectromechanical systems (MEMS) technology the possibility of creating small energy harvesters which can easily be placed in a large variety of scenarios forms one of the main motivations for energy harvesting research. It is emphasised here that, by the term 'size' the authors are referring to the rattle space specifically (as apposed to the size of an attached mass). As one would expect, a reduction in size is often accompanied by a reduction in power output.

2. Broadband performance: for useful amounts of power to be extracted from a LR device it has to be excited close to resonance. Consequently, such devices are poorly suited to harvesting energy from broadband excitations or excitations with time dependent dominant frequencies (characteristics which are typical of many ambient vibration sources).

As a result, the concept of improving energy harvester performance through the intentional introduction of dynamic nonlinearities became a popular topic of research. Among the first to focus on this notion were the works (Mann and Sims, 2009; Cottone, Vocca, and Gammaitoni, 2009; Erturk, Hoffmann, and Inman, 2009) in which the potential benefits of deliberately inducing Duffing-type nonlinearities into energy harvesters were investigated. Of particular interest here is the work of Mann and Sims (2009) in which a device which relied on magnetic levitation was shown to exhibit nonlinearities similar to that of the monostable hardening-spring Duffing oscillator. It was shown that, when under the appropriate excitation conditions, the system was able to converge to either a high or a low energy steady state solution (a well known property of the forced Duffing's equation). It was concluded that, as long as the device was constructed such that it was prone to converge on the high energy solution, the nonlinear device would perform well over a larger bandwidth than LR devices. This idea was investigated further in (Quinn et al., 2011) in which the basins of attraction for the high and low energy solutions were plotted.

A large body of work has also been directed towards the potential benefits of using devices with double-welled potential energy functions. In (Mann and Owens, 2010) it was concluded that through the activation of this 'potential well escape phenomenon' the bandwidth over which energy harvesters perform effectively can be increased. However, in (Masana and Daqaq, 2011) it was shown that, when excited sinusoidally, the ability of interwell dynamics to improve energy harvester performance is very sensitive to excitation amplitude - a conclusion that was also reached in (Erturk and Inman, 2011).

Coupled with this was a body of work which sought to gain a better understanding with respect to the response of energy harvesting devices to Gaussian random excitations (which are thought to form a better approximation of ambient vibrations than monotone sinusoidal excitations). For example, in Gammaitoni, Neri, and Vocca (2009), digital simulations were used to show that the addition of Duffing-type nonlinearities can enhance the power output of noise-driven energy harvesters of both the mono- and bi-stable variety. In (Barton, Burrow, and Clare, 2010) the response of a monostable energy harvester with Duffing-type nonlinearities to random excitations of varying bandwidth was analysed experimentally. It was concluded that, as the bandwidth of the excitation increases, the effect of the nonlinear term on the velocity (and therefore power output) of the device appeared to become 'averaged out' such that it was ineffectual. This was then confirmed analytically in (Daqaq, 2010) where the Fokker-Planck-Kolmogorov (FPK) equation was used to shown that, when under a Gaussian white noise excitation, the addition of Duffing-type nonlinearities into a monostable energy harvester has no benefit with regards to power output. It was subsequently shown in Green et al. (2012a) that this result could be used advantageously as, through employing the hardening-spring nonlinearity, one can reduce the rattle space of an energy harvester without effecting its power output (thus addressing the size issue highlighted earlier in the text).

With regards to randomly excited energy harvesters of the bistable variety, Cottone, Vocca, and Gammaitoni (2009) analysed the response of a bistable device to a Gaussian random excitation with exponential auto correlation. It was concluded that device power output could be enhanced through the activation of noise assisted jumps between energy wells. Additionally, in (Daqaq, 2011b) the Fokker-Planck-Kolmogorov (FPK) equation was used to show that, when under a Gaussian white noise excitation, the mean power output of such a device is independent of the shape of the potential energy function but that, when under an exponentially correlated Gaussian excitation, power output could be maximised through the activation of interwell dynamics. It is also of interest to note that, in a scenario where the the device is excited such that the height of the potential energy barrier oscillates, it has been suggested that the phenomenon of stochastic resonance can be used to enhance power output away from resonance (McInnes, Gorman, and Cartmell, 2008) (although this is not something which is investigated in this paper). Further discussion on the possibility of utilising dynamic nonlinearities to enhance the performance of randomly excited energy harvesters can be found in (Gammaitoni, 2012).

The main question which this paper will try to resolve is: how well can current nonlinear energy harvesting solutions be applied when real ambient vibrations are considered? Although Gaussian white noise

is thought to be a more accurate representation of ambient vibrations than a sinusoidal excitation, it is still an approximation of what an energy harvester would be subjected to in a real world application. Consequently, the aim of this contribution is to gauge how well the conclusions drawn about a device which is excited with Gaussian white noise can be transferred to a scenario where one is attempting to harvest electrical energy from human walking motion or from bridge vibrations (the reasons for choosing these two types of ambient vibration are outlined later). To that end, this paper essentially forms an evaluation of proposed nonlinear energy harvesting techniques when applied to these two very specific excitation cases.

The first part of this work focuses on the simulated response of a monostable nonlinear[1] energy harvesting device. Of specific interest here are the benefits of Duffing-type nonlinearities with regards to device size (as outlined in (Green et al., 2012a)). The second part of this paper will focus on the simulated response of bistable nonlinear energy harvesters - specifically the hypothesis that the useful bandwidth of such devices can be extended by having the system 'escape' from its potential energy well into a high energy solution (Mann and Owens (2010); Erturk and Inman (2011)) or by activating interwell dynamics (Masana and Daqaq (2011)).

Consequently, in this work, acceleration data obtained from the walking motion of 3 individuals, and the vibrations of the mid span of a suspension bridge are used to excite digital simulations of different types of nonlinear energy harvester.

3 Model

Throughout this work the response of SDOF electromagnetic energy harvesters with Duffing-type nonlinearities are studied. Such energy harvesters rely on the oscillation of a magnet relative to coils of wire on the device shell such that a voltage is generated (via Faraday's law). The equation of motion for such a system is given by:

$$m\ddot{z} + (c_m + c_e)\dot{z} + kz + k_3 z^3 = -m y_a(t) \tag{1}$$

where z is the relative displacement between the magnet and the shell of the device, m is the mass of the

[1] Throughout this work the term nonlinear will be used to refer to Duffing-type nonlinearities specifically.

magnet, c_m is the viscous damping due to mechanical losses, k is the linear stiffness, k_3 is the nonlinear stiffness and y_a represents the excitation of the base of the device. The term c_e represents the damping introduced into the system as a consequence of the electromechanical coupling of the device. It can be shown that this term is given by:

$$c_e = \alpha^2 \frac{1}{R_L + R_C} \tag{2}$$

where α is the rate of change of magnetic flux with respect to z and R_L and R_C represent coil and load resistances respectively. This expression for the electromechanical damping relies on the assumptions that the flux displacement relationship is linear (such that α is constant) and that the effects of inductance are negligible - both of which were validated experimentally in (Green et al., 2012a).

The power P delivered to the electrical domain is defined as:

$$P = c_e \dot{z}^2. \tag{3}$$

4 Ambient vibration sources

4.1 Walking motion

The harvesting of energy from human walking motion is often cited as one of the potential applications of energy harvesters. For example, in (Baert et al., 2006) it was proposed that small scale energy harvesters could be used to form part of wearable network of autonomous sensor systems which monitor the health and comfort of an individual. In (Rome et al., 2005) an energy harvesting backpack was developed which, it was suggested, could give freedom to disaster-relief workers who would otherwise need to carry heavy battery packs. This induced an investigation into the effect that such a backpack would have on the human gait (Papatheou et al., 2012). In (Mateu and Moll, 2005) an investigation into the feasibility of harvesting energy from walking motion using piezoelectric film-bending beams placed inside shoes was examined. Furthermore, in reference (Saha et al., 2008) an electromagnetic device was detailed which was designed to supply energy to body worn sensors and other electronic devices. With these potential uses in mind it was decided to investigate the feasibility of applying nonlinear energy harvesting solutions to the scenario of harvesting energy from walking motion.

To acquire a time history of the acceleration due to walking motion, a DC accelerometer was placed on

several participants who were then asked to walk on a tread mill. This data was gathered as part of the work shown in (Papatheou and Sims, 2012) and (Papatheou et al., 2012) (for information about the test procedure the reader is directed towards (Papatheou et al., 2012)). In this case the data from 3 participants walking at 3.6 km/h was analysed. Once 60 seconds of acceleration data had been gathered from each participant, the data was passed through a low pass filter to remove measurement noise (see Figure 1).

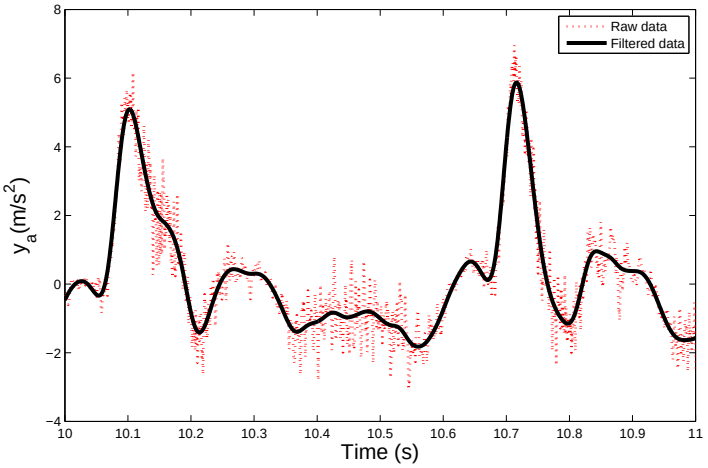

Figure 1: Comparison of raw and filtered walking acceleration data. Dotted and solid lines represent the raw and filtered data respectively.

The frequency content of the resulting excitation signal is shown in Figures 2. With regards to Figure 2 it is interesting to note that, even though they are all walking at the same speed, the frequency content of the signals are unique to each individual. Additionally, the spectrum contains definite 'spikes' while Gaussian white noise has equal power in each frequency. It is also worth noting that, upon studying the excitation histograms in Figure 3 (a), it appears that the acceleration time histories do not have a Gaussian distribution - this is confirmed by the curvature of the quantile plots shown in Figure 3 (b).

The simulated response of a linear device to such an excitation was analysed by using the walking excitation as an input to equation (1) (with $k_3 = 0$) and solving using numerical integration techniques (4th order Runge-Kutta is used throughout this paper). Figure 4 shows a near periodic relative displacement response (z) has been induced from the walking motion of the participants.

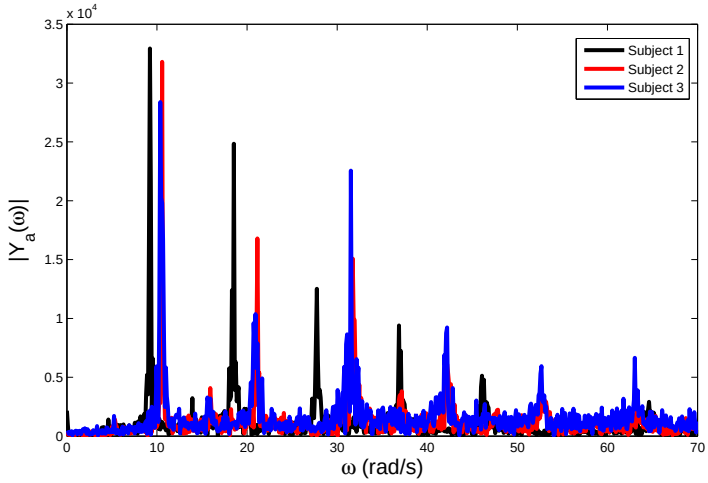

Figure 2: Frequency content of acceleration due to walking motion for subjects 1 2 and 3 (where $Y_a(\omega)$ represents the discrete Fourier transform of $y_a(t)$).

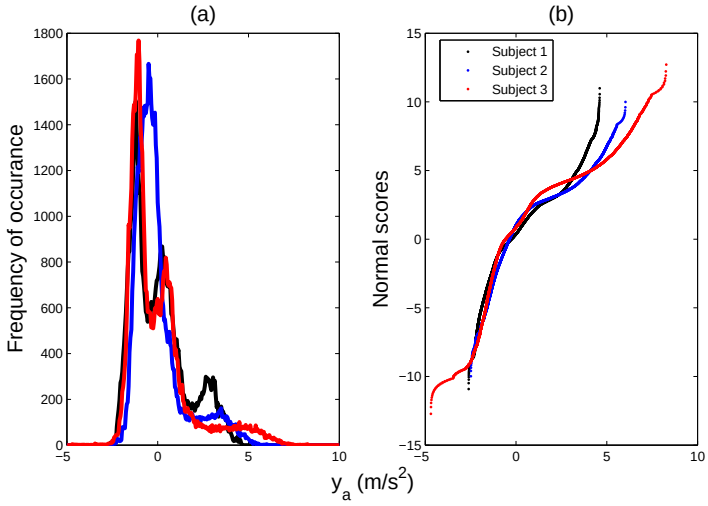

Figure 3: (a) Histograms and (b) quantile plots of acceleration due to walking motion for subjects 1 2 and 3.

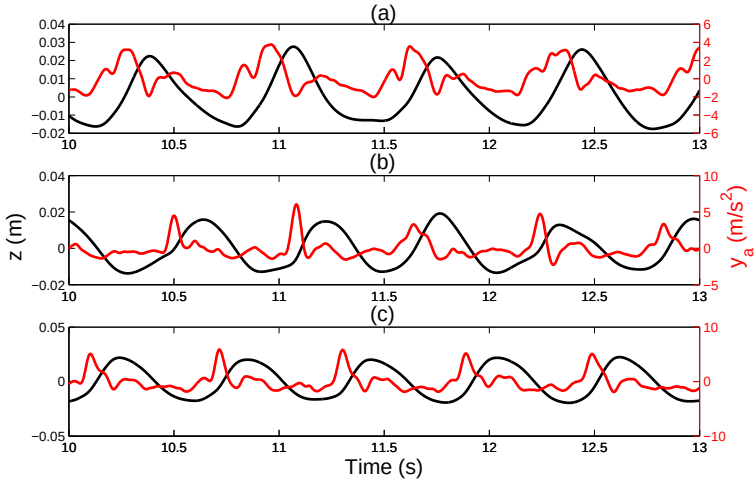

Figure 4: Displacement response of model (black) and acceleration due to walking motion (red) for (a) subject 1, (b) subject 2 and (c) subject 3 where $c_m = c_e = 0.08$ Ns/m , $m = 0.024$ kg and $k_3 = 0$ N/m^3.

4.2 Bridge motion

Alleviating the need for battery replacement, the successful development and implementation of energy harvesters would offer the opportunity for low powered sensors to be placed in hostile or difficult to access environments. Clearly this would be advantageous in a scenario where one is using a large network of sensors to monitor the structural health of a bridge. As a result, bridge vibrations are the second excitation type to be analysed in this paper. The acceleration data used here was gathered from the central span of the Humber bridge, East Yorkshire, England, over a period of two hours [2].

As with the previous example, the acceleration data was passed through a low pass filter to remove measurement noise. Upon studying Figure 5 one can see that, although filtered, the signal still appears to be fairly noisy. This is confirmed when one considers the frequency content of the signal (as shown in Figure 6) where it is shown that, compared with the walking excitation, the power in the bridge excitation signal is dispersed over a greater range of frequencies. Upon consulting the histogram and quantile plot of the data (Figures 7 (a) and (b)), one can see that the bridge excitation also does not appear to have a Gaussian distribution.

Again, using the excitation as an input to the digital model for equation (1), Figure 8 shows that a near periodic relative displacement response (z) is induced.

[2]The authors would like to thank Professor James M.W. Brownjohn from the Civil and Structural engineering department of the University of Sheffield for providing this data.

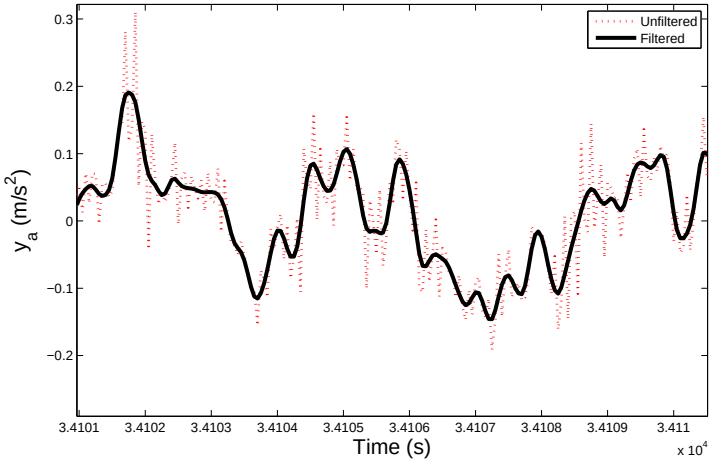

Figure 5: Comparison between raw and filtered acceleration time histories.

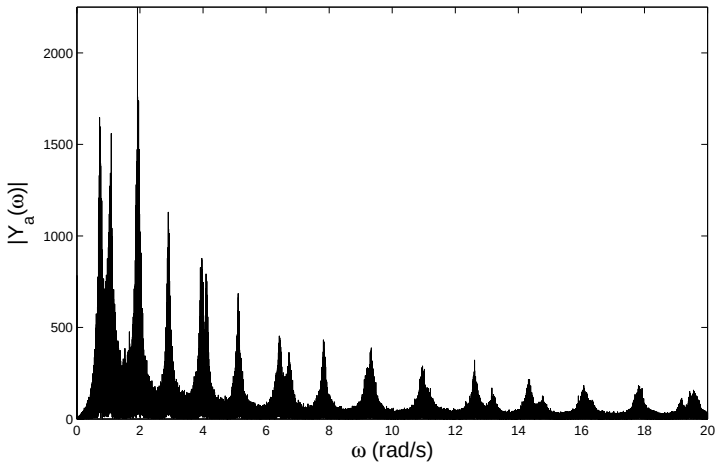

Figure 6: Frequency content of acceleration from bridge motion (where $Y_a(\omega)$ represents the discrete Fourier transform of $y_a(t)$).

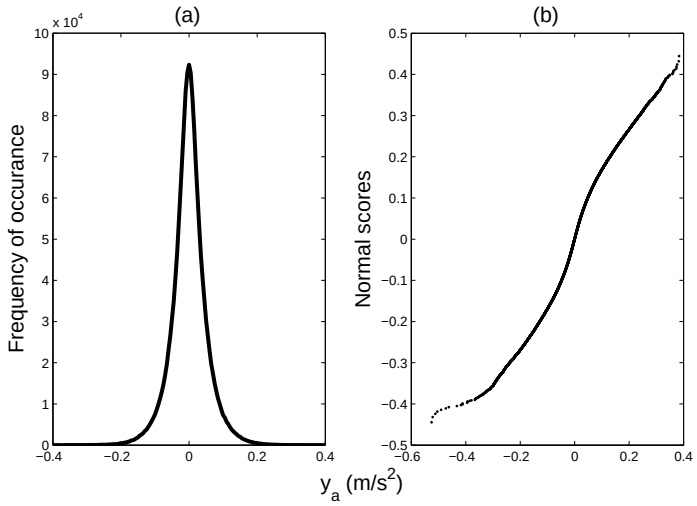

Figure 7: Histogram of acceleration due from bridge motion.

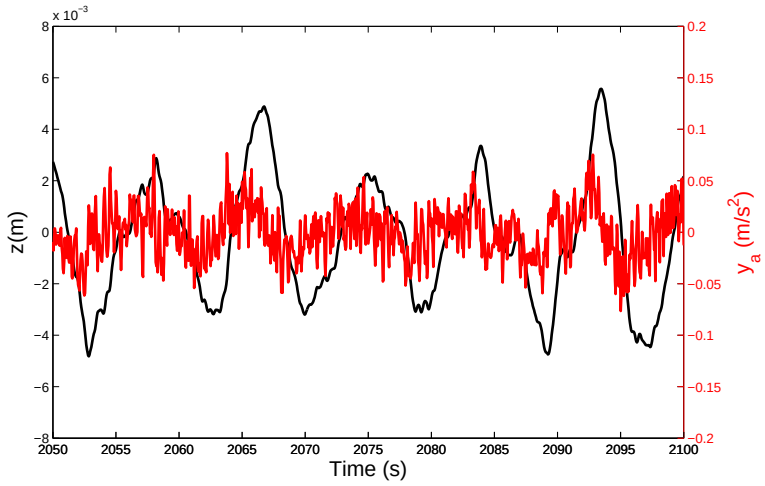

Figure 8: Displacement response of model (blue) and acceleration due to bridge excitation (green) for $c_m = c_e = 0.08$ Ns/m , $m = 0.024$ kg and $k_3 = 0$ N/m^3.

5 Monostable nonlinear energy harvesting

5.1 Device configuration

As mentioned previously, the nonlinear monostable device of interest here was first proposed by Mann and Sims (2009). A schematic of the device is shown in Figure 9. The basic operating principle of this energy harvester is that the centre magnet is held in suspension by the opposing magnetic poles of two outer magnets which are affixed to the shell of the device. In Mann and Sims (2009) it was shown that the restoring force on the centre magnet created by such an arrangement could be accurately modelled

as the force from a nonlinear spring - similar to the hardening-spring Duffing oscillator.

The equation of motion of the the device is as shown in equation (1) where m represents the mass of the *centre* magnet of the device. At this point it is worth noting that, although this model was found to replicate the response of a real device fairly well, in (Green et al., 2012b) it was found that the model was more suitable when the effects of friction were included. The aim of this work however is to investigate the proposed benefits of Duffing-type nonlinearities and so, for the sake of simplicity, friction effects are ignored throughout.

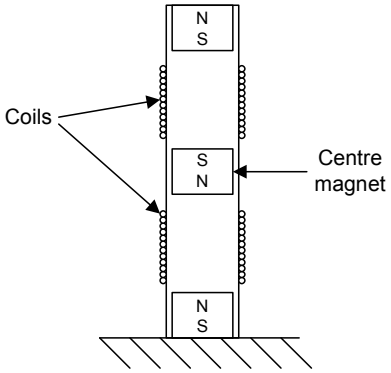

Figure 9: Monostable nonlinear energy harvesting device proposed by Mann and Sims (2009).

5.2 Parameters

In (Green et al., 2012a) a prototype of the monostable device was tested experimentally with an electromagnetic coupling formed by 83 turns of 0.5 mm diameter copper coil. The identified parameters of this device are given in Table 1. While the electromechanical coupling of the device was not optimised, parameter values close to those shown in Table 1 are used throughout this work as they can be considered close to what can be achieved practically.

Parameter	Value	Units
m	0.0236	kg
c_m	0.088	Ns/m
c_e	0.083	Ns/m

Table 1: Parameters of monostable nonlinear device analysed in (Green et al., 2012a).

5.3 Simulated response to walking motion

When developed initially, it was supposed that the deliberate introduction of the nonlinear spring term would allow the nonlinear monostable device to function over a larger bandwidth of frequencies than a LR energy harvester. Although it is now thought that this is not the case (see (Daqaq, 2010) and (Green et al., 2012a)) it has since been shown that, when under Gaussian white noise excitations, the nonlinear spring term can be used to reduce the rattle space of the device without effecting its power output (Green et al., 2012a). The aim here then, is to identify whether these findings can be extended to the case where the device is excited by human walking motion.

Using the walking excitation data of subject 2 as an input to the digital model of the device, Figure 10 shows the variation of expected power delivered to the electrical domain (defined as $P = c_e\dot{z}^2$) and the displacement variance of the device for different values of linear and nonlinear stiffness (k and k_3). With regards to the simulated response of the linear device (solid lines on Figure 10) the first thing to be noted is that the device achieves maximum power output and, consequently, maximum displacement, when its natural frequency is tuned to the dominant frequency of excitation (a rather intuitive result). As k is increased one can see an increase in power output when the device is tuned to the second harmonic of the excitation ($k \approx 11$ N/m). With the nonlinear spring term set to 5000 N/m^3 (dashed lines on Figure 10) one can see that the optimum value of k (with regards to power output) has been reduced. This is a consequence of the 'skewing' effect that is caused by hardening spring nonlinearities - the nonlinear spring term has increased the resonant frequency of the device such that a lower value of linear stiffness is now required to tune the device to the dominant frequency of excitation. The key finding from these results are that, although the addition of the nonlinear stiffness term has reduced the displacement of the device, this reduced displacement has been accompanied by a reduction in the power output. This is contrary to the findings shown in (Green et al., 2012a) thus highlighting the potential difficulties involved with transferring findings developed under the assumption of a Gaussian white noise excitation to a real world energy harvesting scenario. Similar results to that shown in Figure 10 were found when the walking data from the other participants were used. The conclusions drawn from these results were also found to be independent of the damping levels used in each simulation.

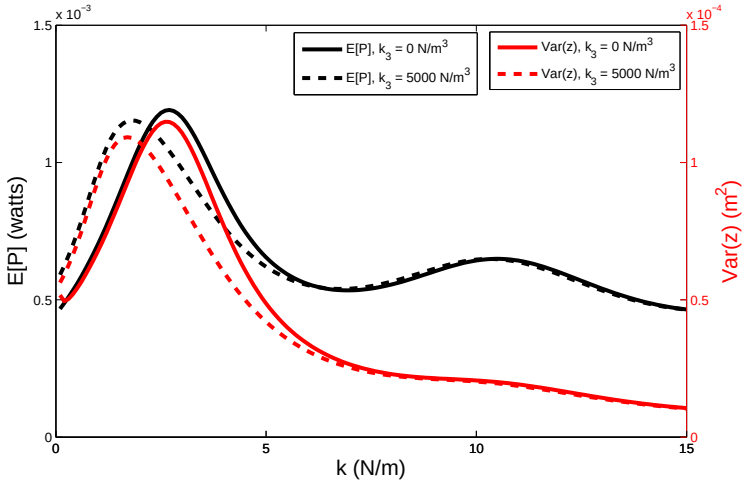

Figure 10: Simulated response of device to excitation from subject 2 walking motion: the variation of displacement and power with linear stiffness where the solid and dashed lines represent cases where $k_3 = 0$ and 5000 N/m^3 respectively. All other parameters are as shown in Table 1.

The aim of the next phase of the analysis was to identify the effect of the nonlinear spring term on the response of the device when it is tuned such that its power output is maximised. Figure 11 shows the variation of expected power and displacement variance for different values of k_3 where, for every data point, k was chosen such the power output of the device was maximised. Consequently, the notation k_{opt} and P_{opt} is used to denote the optimum linear stiffness and resulting power output while $\mathrm{Var}(z|P_{opt})$ is used to represent the displacement variance of the device given that the device has been optimised with regards to power output. Clearly, any benefit with regards to device rattle space has come at the expense of power output.

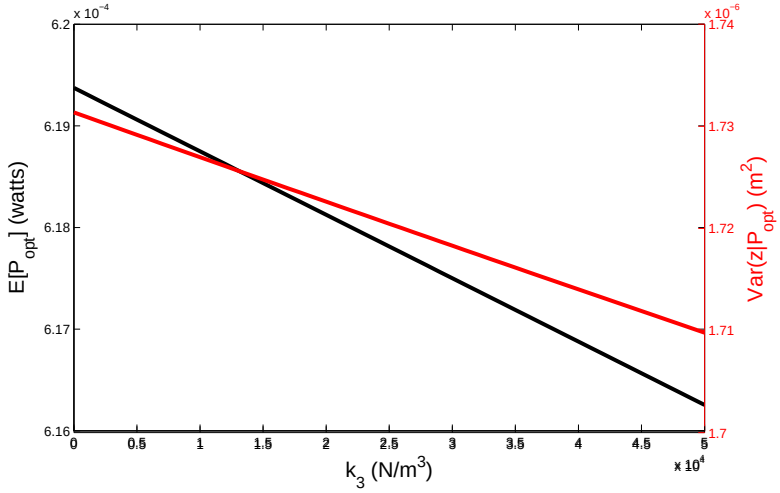

Figure 11: Simulated response of device to excitation from subject 2 walking motion: the variation of displacement and power with nonlinear stiffness where $k = k_{opt}$. All other parameters are as shown in Table 1.

5.4 Simulated response to bridge motion

In the previous section it was shown that, for the case of walking motion, it is difficult to realise the benefits of Duffing-type nonlinearities without harming the maximum power output of the device. The aim of the current section then is to carry out a similar analysis using the bridge acceleration data as the excitation. The results of this investigation are shown in Figure (12) where it can be seen that, once again, any benefits with regards to displacement variance have come at the expense of reduced power output. Additionally, as with the walking motion case, the optimum linear stiffness has been reduced as a consequence of the addition of the nonlinear stiffness term. With the dominant frequencies of the bridge excitation being so low, this has resulted in the optimum level of linear stiffness approaching zero.

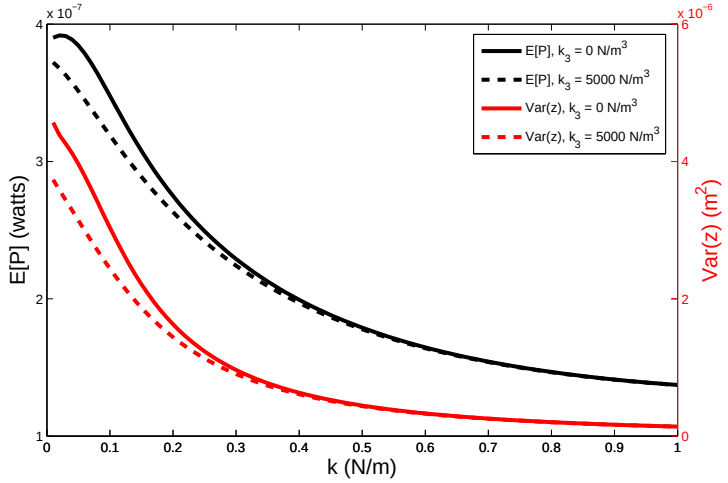

Figure 12: Simulated response of device to bridge excitation: the variation of displacement and power with linear stiffness where the solid and dashed lines represent cases where $k_3 = 0$ and 5000 N/m^3 respectively. All other parameters are as shown in Table 1.

As before, the variation of expected power and displacement variance was plotted for different values of nonlinear stiffness where, at every data point, the linear stiffness was chosen to maximise power output (Figure 13). Once again it is clear that, while reducing the displacement variance, the introduction of the nonlinear spring term also reduces power output.

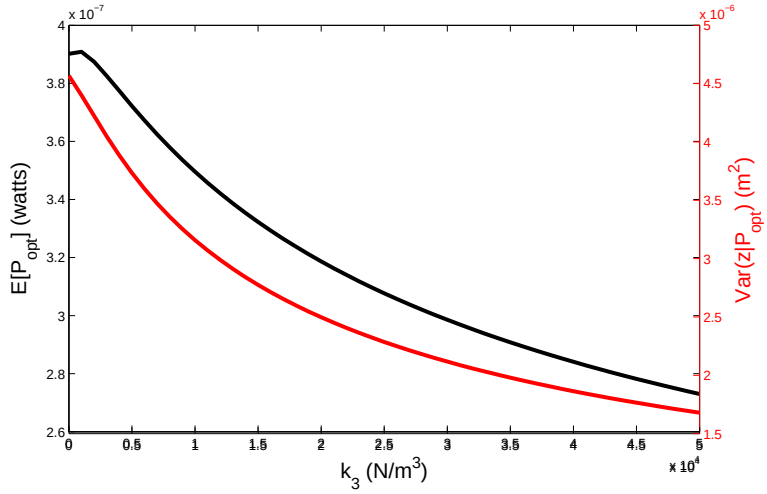

Figure 13: Simulated response of device to bridge excitation: the variation of displacement and power with nonlinear stiffness where $k = k_{opt}$. All other parameters are as shown in Table 1.

6 Bistable nonlinear energy harvesting

Having investigated the application of a monostable nonlinear energy harvesting solution, attention is now directed towards bistable energy harvesters. An example of a bistable piezoelectric device shown in Figure 14. This consists of a cantilever beam with a magnet attached at one end which is orientated such that it repels another magnet which is attached to the shell of the device. The design is such that, as a result of the magnetic repulsion force, the beam has two equilibrium positions (as indicated by the dashed lines in Figure 14) thus making it bistable. For detailed analyses of such a device the reader is directed towards references (Cottone, Vocca, and Gammaitoni, 2009) and (Erturk and Inman, 2011).

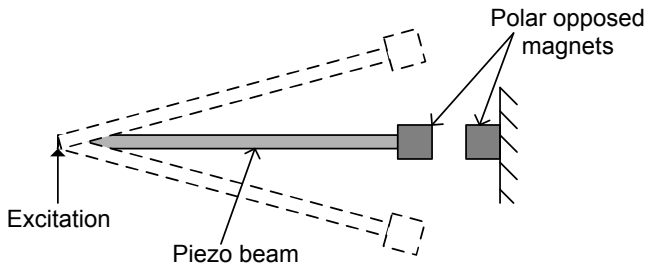

Figure 14: Example of a piezoelectric bistable energy harvester.

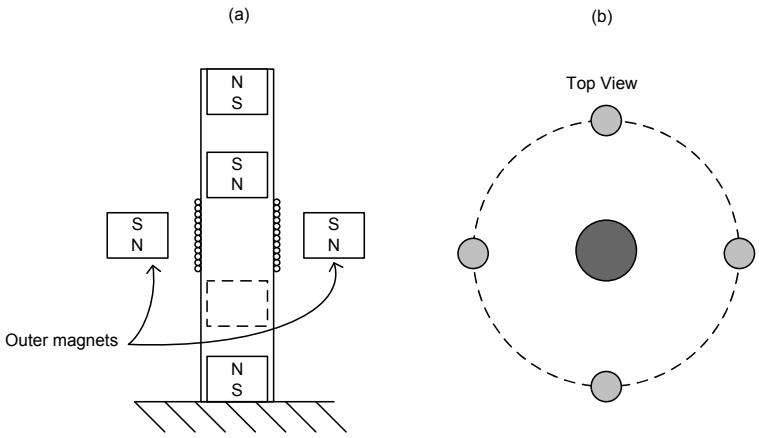

Figure 15: Bistable electromagnetic energy harvester proposed in Mann and Owens (2010).

An alternative construction of bistable energy harvester was developed in Mann and Owens (2010) (see Figure 15). This device is essentially a bistable version of the Mann and Sims energy harvester (which has been the main focus of this paper thus far). Consequently, assuming that the device being investigated here is similar in construction to that shown in Figure 15, parameter values similar to those shown in Table 1 are used in the subsequent investigation.

The equation of motion of such a device is often approximated as:

$$m\ddot{z} + c\dot{z} - kz + k_3 z^3 + F_e = -my_a. \tag{4}$$

It should be noted that equation (4) now contains a negative value of k such that, upon the appropriate selection of k and k_3, a device with a bistable potential is created.

6.1 Simulated response to walking motion

As mentioned previously, it is clear that the power in the walking excitation signal is distributed over a relatively large range of frequencies. The purpose of this investigation then is to identify whether a bistable device can harvest energy over a larger bandwidth and therefore outperform a linear resonant device. Figure 16 shows how the simulated power delivered to the electrical domain varied with different values of k and k_3. Interestingly, the optimum amount of power is harvested when k is positive and k_3 approaches zero - in other words, the monostable linear device out performs the nonlinear bistable device. This can be seen more clearly in Figure 17 which shows two cross sections taken from the contour plot of Figure 16.

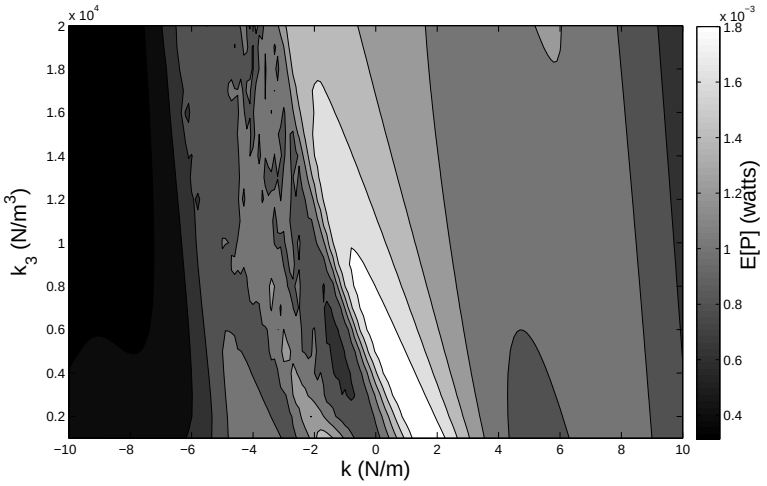

Figure 16: Walking excitation (subject 1): variation of power delivered to the electrical domain with changes in k and k_3. All other parameters are as shown in Table 1.

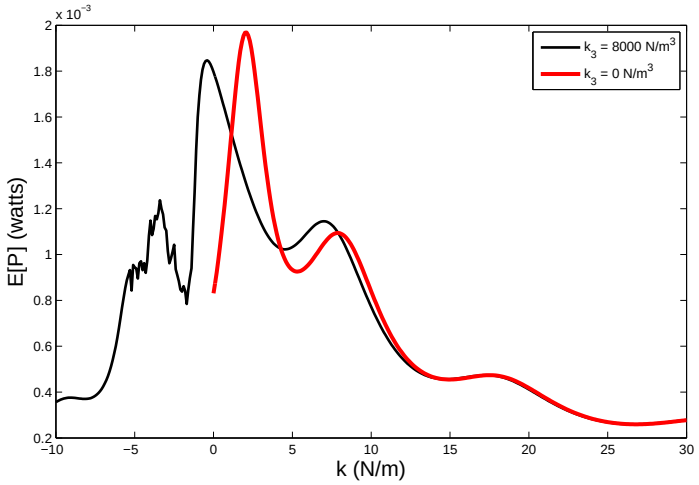

Figure 17: Walking excitation (subject 1): variation of power delivered to the electrical domain with changes in k where the black and red lines represent simulations where $k_3 = 8000$ and 0 N/m^3 respectively. All other parameters are as shown in Table 1.

The first point to note with regards to Figure 17 is that the power output in the region where $k = -10$ and $k_3 = 8000$ is relatively small. In an effort to understand why, a phase portrait for the system with the afore mentioned values of linear and nonlinear stiffness was plotted (Figure 18). It is clear that the system is entrapped in one energy well and is unable to jump into the other. Figure 19 shows a phase portrait for the case when $k = -3$ and $k_3 = 8000$. Interwell dynamics have been activated although, upon consulting Figure 16, it is clear that this has yielded little benefit with regards to power output. Finally, Figure 20 shows the phase portrait for the linear monostable case. To summarise then, the linear monostable device has outperformed the nonlinear bistable. Again, similar results were found for all three subjects.

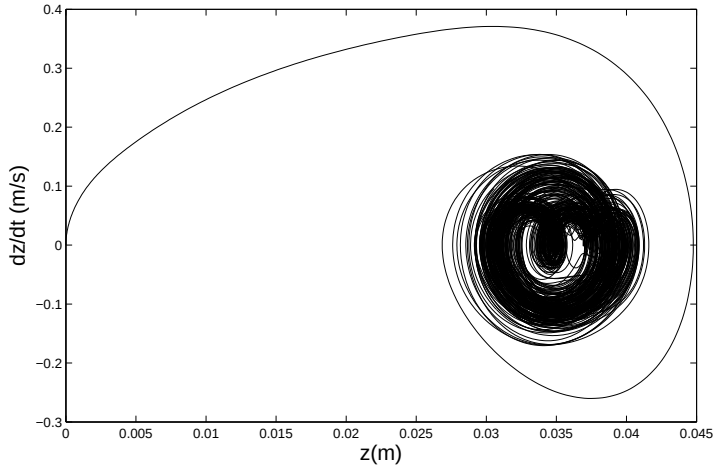

Figure 18: Phase portrait of bistable oscillator under walking excitation (subject 1) where k = -10 N/m and k_3 = 8000 N/m^3 and all other parameters are as shown in Table 1.

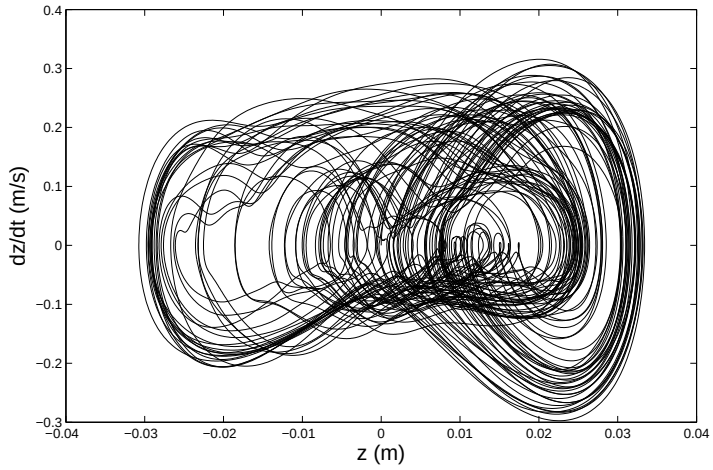

Figure 19: Phase portrait of bistable oscillator under walking excitation (subject 1) where k = -3 N/m and k_3 = 8000 N/m^3 and all other parameters are as shown in Table 1.

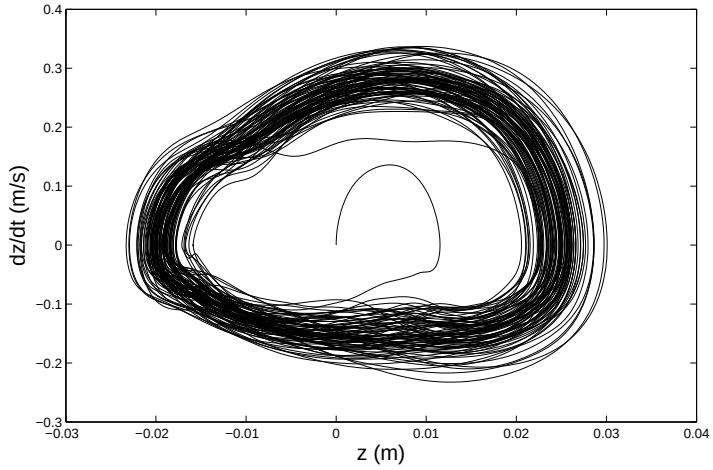

Figure 20: Phase portrait of bistable oscillator under walking excitation (subject 1) where k = -2.5 N/m and $k_3 = 0$ N/m^3 and all other parameters are as shown in Table 1.

6.2 Simulated response to bridge motion

Analysing the simulated response of a bistable device to the bridge excitation, the contour plot in Figure 21 was realised. Interestingly in this case, there are regions where the bistable device produces a power output similar to that of the linear monostable device. Figure 22 shows that, when $k_3 = 2000$, there is a region where having a negative value of k results in a power output very close to that of the optimum linear case.

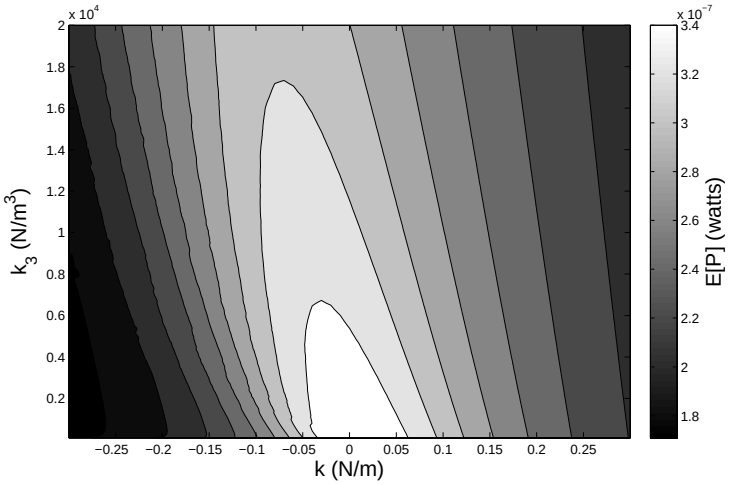

Figure 21: Bridge excitation: variation of power delivered to the electrical domain with changes in k and k_3. All other parameters are as shown in Table 1.

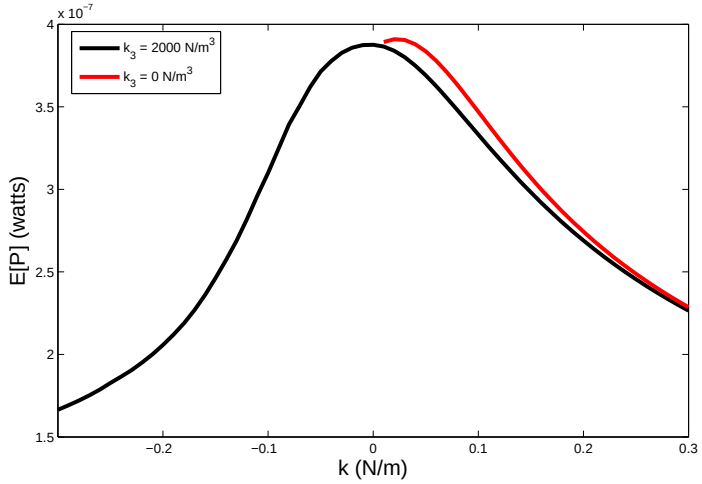

Figure 22: Bridge excitation: variation of power delivered to the electrical domain with changes in k where the black and red lines represent simulations where $k_3 = 2000$ and 0 N/m^3 respectively. All other parameters are as shown in Table 1.

Again, to further understand the dynamics of the device, phase portraits were plotted using different values of linear and nonlinear stiffness. Setting $k = -0.1$ and $k_3 = 2000$ such that device was in a 'high power' region of Figure 16 the phase portrait shown in Figure 23 was realised. The device is clearly demonstrating interwell dynamics - an interesting result as, with regards to the walking excitation case, this seemed to harm device performance. This result shows that the benefits of inducing interwell dynamics are certainly excitation specific.

Moving into one of the relatively low power regions ($k = -0.2$ and $k_3 = 2000$) then, as shown in Figure 24, it is clear that the device is entrapped in one energy well from which it is is unable to escape. It is also interesting to note that only a small alteration in linear stiffness (≈ 0.1 N/m) was required to change from a device which can active interwell dynamics to one which cannot. This suggests that, if one did want to create a device capable of jumping between energy wells, one would have to tune its linear stiffness very precisely. In fact, this is exactly what is required if attempting to tune the natural frequency of a linear device to the dominant frequency of excitation - therefore prompting one to question the value in selecting a bistable energy harvester over a linear resonant energy harvester.

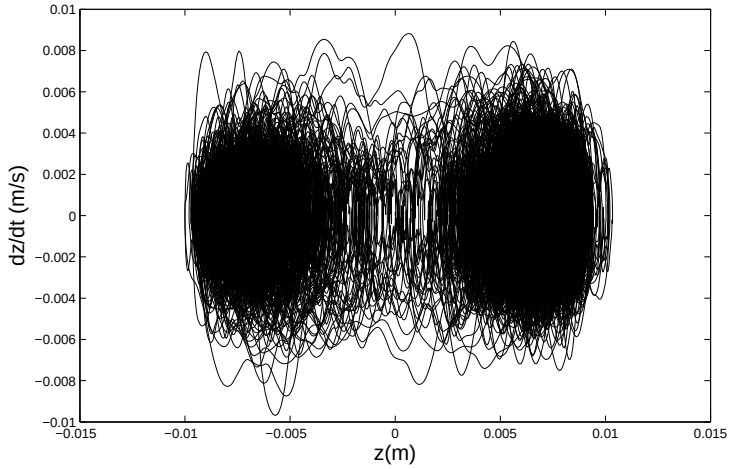

Figure 23: Phase portrait of bistable oscillator under bridge excitation where k = -0.1 N/m and k_3 = 2000 N/m^3 and all other parameters are as shown in Table 1.

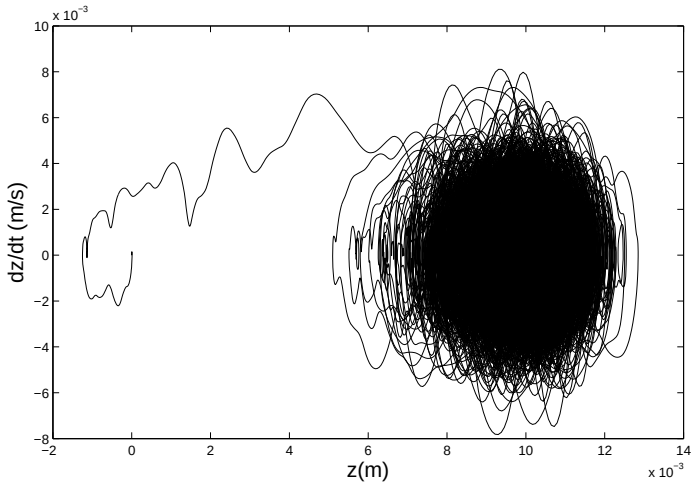

Figure 24: Phase portrait of bistable oscillator under bridge excitation where k = -0.2 N/m and k_3 = 2000 N/m^3 and all other parameters are as shown in Table 1.

7 Future work and discussion

Something which is touched on in this work but not discussed thoroughly is the fact that both types of ambient excitation investigated in this paper have very low dominant frequencies. Constructing a small device to harvest energy from such frequencies would be difficult as, to achieve such a low natural frequency, one would require a large mass or weak restoring force. While the authors are aware of devices which are specifically designed for such purposes (see (Liu et al., 2012) and (Zhang and Cai, 2012)) their reported natural frequencies are not as low as the dominant frequencies of the excitations

shown in this paper.

The issue of low frequency energy harvesting brings one to question the suitability of electromagnetic and piezoelectric conversion mechanisms. The circuitry of piezoelectric devices are usually modelled as containing a capacitance and load resistance (Masana and Daqaq, 2011). As it is known that a series combination of capacitor and resistor creates a high pass filter, it is intuitive to suggest that a piezoelectric device would be poorly suited to harvesting energy from low frequencies. On the other hand, electromagnetic devices whose circuitry is often modelled as a series combination of inductor and resistor would not suffer from such issues as, even if the inductance was large (which is unlikely in a small device), the circuit would be acting as a low pass filter - thus allowing it to harvest electrical energy from low frequencies. It is also worth noting that, under certain conditions, the nature of the electromechanical coupling used may alter the effect that Duffing-type nonlinearities have on device performance. For example, in (Daqaq, 2011a) it is shown that when the time constant of the device circuity is close to that of the device dynamics then the introduction of the afore mentioned nonlinearities can reduce the power output of a white noise-excited device.

With regards to nonlinear energy harvesting from low frequency vibrations, some recent works (Cohen, Bucher, and Feldman, 2012; Masana and Daqaq, 2012) have suggested that Duffing-type nonlinearities could be introduced such that the device response contained subharmonics which would help it harvest energy from below its natural frequency. This has not been explored in the present study.

The final point worthy of discussion is with regards to bistable energy harvesters which are designed to exhibit interwell dynamics. An interesting point that was raised in (Erturk and Inman, 2011) as well as (Barton, Burrow, and Clare, 2010) is that, even if power output could be improved through the activation of interwell dynamics, the unperiodic nature of the instantaneous power would make it difficult to collect and store the electrical energy. This is certainly an area in which further research could be directed.

8 Conclusions

The aim of this paper was to assess whether nonlinear energy harvesting solutions developed under the assumption of Gaussian white noise ambient vibrations can be applied ubiquitously in the real world.

Two possible ambient vibration sources were considered (human walking motion and bridge vibrations). Using real vibration measurements in simulations of idealised energy harvesters it was shown that, although the benefits of deliberately inducing dynamic nonlinearities into such devices has been shown for the case of Gaussian white noise excitations, the same benefits could not be realised for the real excitation conditions. Consequently, the main conclusion of this paper is to demonstrate that universally applicable nonlinear energy harvesting solutions cannot be realised without a more careful consideration of the nature of ambient vibrations. This certainly does not mean that the works referred to in this paper are ineffectual - they have greatly improved our understanding of how dynamic nonlinearities effect the performance of randomly excited energy harvesters. The aim of this paper is certainly not to criticise these works but to suggest that, for the development of energy harvesting solutions to be successful, the nature of ambient vibration sources will have to be analysed in more detail. This is something which may be possible to accomplish through use of the 'real vibration database' outlined in (Neri et al., 2012). It may also be of interest to analyse whether results realised using band-limited exponentially-correlated random excitations (which are often considered a better approximation of ambient excitations than white noise) can be successfully applied in real-world scenarios.

The second main contribution of this paper is to emphasise that the harvesting of energy from ambient vibration sources will likely require the development of devices which are capable of operating at very low frequencies. It is stated here that electromagnetic energy harvesters will be better suited to this type of problem as the circuitry of piezoelectric devices are known to act as a high pass filters - thus removing low frequency electrical signals. There is certainly much scope in investigating whether dynamic nonlinearities can be used to aid the harvesting of energy from low frequency vibrations.

9 Acknowledgements

The authors would like to thank Professor James M.W. Brownjohn from the Civil and Structural engineering department of the University of Sheffield for providing vibration data from the midspan of the Humber bridge.

This study was supported by a grant from an EPSRC studentship (grant reference no. EP/H020764/1).

References

Baert, K., Gyselinckx, B., Torfs, T., Leonov, V., Yazicioglu, F., Brebels, S., Donnay, S., Vanfleteren, J., Beyne, E., and Van Hoof, C., 2006. "Technologies for highly miniaturized autonomous sensor networks." Microelectronics Journal, 37(12):1563–1568.

Barton, D., Burrow, S., and Clare, L., 2010. "Energy harvesting from vibrations with a nonlinear oscillator." Journal of Vibration and Acoustics, Transactions of the ASME, 132(2):0210091–0210097.

Beeby, S.P., Tudor, M.J., and White, N.M., 2006. "Energy harvesting vibration sources for microsystems applications." Measurement Science and Technology, 17(12):R175.

Cohen, N., Bucher, I., and Feldman, M., 2012. "Slow-fast response decomposition of a bi-stable energy harvester." Mechanical Systems and Signal Processing.

Cottone, F., Vocca, H., and Gammaitoni, L., 2009. "Nonlinear energy harvesting." Physical Review Letters, 102(8).

Daqaq, M.F., 2010. "Response of uni-modal duffing-type harvesters to random forced excitations." Journal of Sound and Vibration, 329(18):3621–3631.

Daqaq, M., 2011a. "On intentional introduction of stiffness nonlinearities for energy harvesting under white Gaussian excitations." Nonlinear Dynamics:1–17.

Daqaq, M.F., 2011b. "Transduction of a bistable inductive generator driven by white and exponentially correlated Gaussian noise." Journal of Sound and Vibration, 330(11):2554 – 2564.

Erturk, A., Hoffmann, J., and Inman, D., 2009. "A piezomagnetoelastic structure for broadband vibration energy harvesting." Applied Physics Letters, 94(25). Cited By (since 1996) 85.

Erturk, A. and Inman, D., 2011. "Broadband piezoelectric power generation on high-energy orbits of the bistable Duffing oscillator with electromechanical coupling." Journal of Sound and Vibration, 330(10):2339–2353.

Gammaitoni, L., 2012. "There's plenty of energy at the bottom (micro and nano scale nonlinear noise harvesting)." Contemporary Physics, 53(2):119–135. Cited By (since 1996) 1.

Gammaitoni, L., Neri, I., and Vocca, H., 2009. "Nonlinear oscillators for vibration energy harvesting." Applied Physics Letters, 94(16).

Green, P.L., Worden, K., Atallah, K., and Sims, N.D., 2012a. "The benefits of Duffing-type nonlinearities and electrical optimisation of a mono-stable energy harvester under white Gaussian excitations." Journal of Sound and Vibration, 331(20):4504 – 4517.

Green, P., Worden, K., Atallah, K., and Sims, N., 2012b. "The effect of Duffing-type non-linearities and Coulomb damping on the response of an energy harvester to random excitations." Journal of Intelligent Material Systems and Structures.

Liu, H., Lee, C., Kobayashi, T., Tay, C., and Quan, C., 2012. "A new S-shaped MEMS PZT cantilever for energy harvesting from low frequency vibrations below 30 Hz." Microsystem Technologies, 18(4):497–506.

Mann, B. and Owens, B., 2010. "Investigations of a nonlinear energy harvester with a bistable potential well." Journal of Sound and Vibration, 329(9):1215–1226.

Mann, B.P. and Sims, N.D., 2009. "Energy harvesting from the nonlinear oscillations of magnetic levitation." Journal of Sound and Vibration, 319(1-2):515–530.

Masana, R. and Daqaq, M., 2011. "Relative performance of a vibratory energy harvester in mono- and bi-stable potentials." Journal of Sound and Vibration, 330(24):6036–6052.

Masana, R. and Daqaq, M., 2012. "Energy harvesting in the super-harmonic frequency region of a twin-well oscillator." Journal of Applied Physics, 111(4).

Mateu, L. and Moll, F., 2005. "Optimum piezoelectric bending beam structures for energy harvesting using shoe inserts." Journal of Intelligent Material Systems and Structures, 16(10):835–845.

McInnes, C., Gorman, D., and Cartmell, M., 2008. "Enhanced vibrational energy harvesting using nonlinear stochastic resonance." Journal of Sound and Vibration, 318(4-5):655–662.

Mitcheson, P., Green, T., Yeatman, E., and Holmes, A., 2004. "Architectures for vibration-driven micropower generators." Journal of Microelectromechanical Systems, 13(3):429–440.

Neri, I., , Travasso, F., Mincigrucci, R., Vocca, H., Orfei, F., and Gammaitoni, L., 2012. "A real vibration database for kinetic energy harvesting application." Journal of Intelligent Material Systems and Structures.

Papatheou, E., Green, P.L., Racic, V., JMW, B., and Sims, N.D., 2012. "A short investigation of the effect of an energy harvesting backpack on the human gait." Proceedings of SPIE 2012, Smart Structures/NDE, San Diego, California.

Papatheou, E. and Sims, N., 2012. "Developing a hardware in-the-loop simulator for a backpack energy harvester." Journal of Intelligent Material Systems and Structures, 23(7):827–835.

Quinn, D., Triplett, A., Bergman, L., and Vakakis, A., 2011. "Comparing linear and essentially nonlinear vibration-based energy harvesting." Journal of Vibration and Acoustics, Transactions of the ASME, 133(1).

Rome, L., Flynn, L., Goldman, E., and Yoo, T., 2005. "Biophysics: Generating electricity while walking with loads." Science, 309(5741):1725–1728.

Saha, C., O'Donnell, T., Wang, N., and McCloskey, P., 2008. "Electromagnetic generator for harvesting energy from human motion." Sensors and Actuators, A: Physical, 147(1):248–253.

Stephen, N., 2006. "On energy harvesting from ambient vibration." Journal of Sound and Vibration, 293(1-2):409 – 425.

Williams, C.B. and Yates, R.B., 1996. "Analysis of a micro-electric generator for microsystems." Sensors and Actuators A: Physical, 52(1-3):8 – 11.

Zhang, Y. and Cai, C., 2012. "A retrofitted energy harvester for low frequency vibrations." Smart Materials and Structures, 21(7).